Plant Protein Amyloid Fibrils for Multifunctional Sustainable Materials

Journal Article

Author(s):
Li, Ting; Zhou, Jiangtao; Peydayesh, Mohammad; Yao, Yang; Bagnani, Massimo; Kutzli, Ines; Chen, Zhengxing; Wang, Li; Mezzenga, Raffaele

Publication date:
2023-04

Permanent link:
https://doi.org/10.3929/ethz-b-000596016

Originally published in:
Advanced Sustainable Systems 7(4), https://doi.org/10.1002/adsu.202200414

ADVANCED SUSTAINABLE SYSTEMS
www.advsustainsys.com

Plant Protein Amyloid Fibrils for Multifunctional Sustainable Materials

Ting Li, Jiangtao Zhou, Mohammad Peydayesh, Yang Yao, Massimo Bagnani, Ines Kutzli, Zhengxing Chen, Li Wang, and Raffaele Mezzenga**

Artificial functional materials based on amyloid fibrils are proven to be a promising strategy toward functional materials. However, scaling-up applications present sustainability concerns, as animal proteins are the main sources for fabricating amyloid fibrils. Plant-protein-based amyloid fibrils, a more sustainable alternative to animal proteins, are attracting increasing interests as building blocks in functional materials. Herein, 11 different sources from a wide range of plants are evaluated, and a comprehensive analysis of seven species of plant proteins, including kidney bean, black bean, cowpea, mung bean, chickpea, lentil, and pumpkin seed, with an excellent ability to form fibrils, is presented. A universal strategy for a diversity of plant protein extraction and fibrillization is applied. Flexible fibrils with a persistence length of ≈100 nm and rigid fibrils of several micrometers are discovered in 7S/8S and 11S subunits dominated protein, respectively. Structural evolution toward the β-sheet content on these proteinaceous assemblies is characterized by thioflavin T (ThT) intensity, circular dichroism (CD) spectra, attenuated total reflectance-Fourier transform infrared (ATR-FTIR) spectra, and typical wide angle X-ray scattering (WAXS) spectra. Finally, their multifunctional applications are further explored and proven that these sustainable protein amyloids demonstrate excellent performance in renewable and degradable bioplastics, and in water purification membranes for heavy metal removal.

1. Introduction

Amyloid fibrils are fibrillar proteinaceous assemblies traditionally perceived as pathological aggregates related to human neurodegenerative diseases.[1] However, it has gradually been discovered that the amyloidogenic propensity is an intrinsic property of many proteins.[2] Up to now, a wide variety of peptides or proteins,[3] containing amyloidogenic regions, have been determined to be capable of assembling into amyloid fibrils under suitable conditions, most commonly at low pH and high temperature.[4] Due to their unique features at multiple scales, amyloid fibrils as building blocks in functional materials have been attracting great attention in recent years,[5] such as in controlled drug delivery platforms,[6] biosensors,[7] and cell culture scaffolds.[8] Food protein amyloid fibrils, as a widely available source, have inspired researchers to explore their potential for advanced functional materials.[9] For example, lysozyme and β-lactoglobulin amyloid fibrils[10] showed multiple functional applications, including antibacterial hydrogels,[11] delivery systems for nanosized iron,[12] and versatile adsorbents for water purification.[13] To date, amyloid fibrils self-assembly from animal proteins has a well-established formation mechanism.[9] However, the usage of plant protein amyloid fibrils is more environmentally-friendly and sustainable for future scaled-up food and material applications. Despite the environmental abundance and availability of plants, proteins from plant sources remain poorly studied for amyloid fibrillization.[14] Indeed, limited literature is available on the structural characterization and applications of plant-based fibrils, probably attributable to the complex composition and low purity of plant proteins.[10a,15] Due to rapid global population growth and major environmental problems, the demand for developing sustainable and affordable amyloid building blocks for manufacturing functional materials has become increasingly critical. Therefore, evaluating fibrillation propensity from plant sources and further exploring their potential material functionalities constitute challenging and important tasks.

Amyloid fibrils are characterized by typical cross β-structures which, however, exhibit a large degree of mesoscopic polymorphism,[16] even with the same polypeptides, due

T. Li, Z. Chen, L. Wang
School of Food Science and Technology
National Engineering Research Center for Cereal Fermentation and Food Biomanufacturing
Key Laboratory of Carbohydrate Chemistry and Biotechnology Ministry of Education
Jiangnan University
Lihu Road 1800, Wuxi 214122, China
E-mail: wangli0318@jiangnan.edu.cn
T. Li, J. Zhou, M. Peydayesh, Y. Yao, M. Bagnani, I. Kutzli, R. Mezzenga
Department of Health Sciences and Technology
ETH Zurich
Zurich 8092, Switzerland
E-mail: raffaele.mezzenga@hest.ethz.ch
R. Mezzenga
Department of Materials
ETH Zurich
Zurich 8093, Switzerland
The ORCID identification number(s) for the author(s) of this article can be found under https://doi.org/10.1002/adsu.202200414.

DOI: 10.1002/adsu.202200414

to the dynamic state of the amyloid.[9] The same protein under different fibrillization conditions, such as concentration,[17] pH,[18] ionic strength,[19] as well as denaturing agents,[20] might present substantial mesoscopic differences, thus impeding comparisons between different protein sources. Furthermore, only limited literature exists on developing a universal protein extraction method and fibrillization condition from a wide range of plants.[15] To the best of our knowledge, extant literature is primarily focused on proteins from legumes (i.e., most commonly soybean[21]), and cereals (i.e., recently unraveled rice[22] and oat[23]). Only a few investigations demonstrated the feasibility of oilseeds, edible seeds, and pseudocereals.[9,15] Moreover, the field of plant-based amyloid fibrils applied for functional materials remains largely unestablished. This work focused on fibrils formation, characterization, and application from a broad spectrum of plants, including legumes, cereals, oilseeds, and pseudocereals. We first performed a universal extraction and fibrillization method for a wide range of plant proteins, including black bean, pumpkin seed, kidney bean, cowpea, mung bean, chickpea, lentil, millet, chia seed, quinoa, and buckwheat. We further comprehensively analyzed the structural details of seven kinds of manufactured amyloid fibrils, and explored the potential applications of these plant-based amyloid fibrils in multifunctional materials, including hydrogel fabrication, water purification membranes, and bioplastics.

2. Results and Discussion

2.1. Protein Extraction from Different Plant Sources

Many technologies such as acids, alkaline, salt, and enzymes treatments have been proposed to extract and recover protein isolates from plant seeds.[24] Due to their pH-dependent surface charge that affects their water solubility, the majority of plant proteins, including albumin, globulin, prolamin, and glutelin, are normally soluble in alkaline solution, with a maximum extractability at pH 8–12, and precipitate at acidic conditions, usually at pH 4–5.[25] Consequently, we propose to extract plant proteins using a universal alkaline extraction method for a wide range of plant proteins to produce a suitable raw material for fibrillization, as shown in **Figure 1**a, and then precipitate them at their isoelectric point (AE-IP), approximately pH 4.5, depending on the plant used. In general, the protein yield increases upon raising the pH value of extraction dispersion within an appropriate range. However, the purity, solubility, functionality, and nutritional profile of the extracted protein are influenced negatively at very high pH (usually above 10) due to starch contamination and denaturation.[26] Therefore, to achieve high recovery and quality of proteins and retain their nutritional benefits, a milder alkaline solution (pH 8/10) was used in this study, which was optimized after comparing results from the literature[27] and our previous studies.[28] The legume

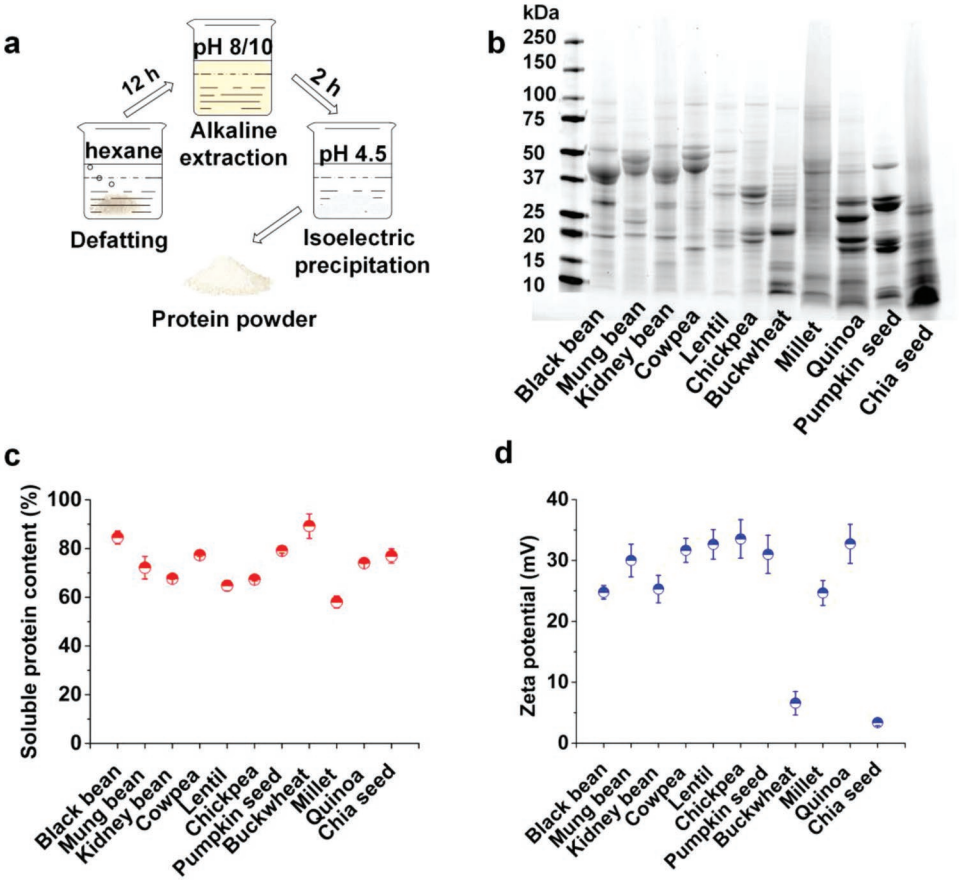

Figure 1. Extraction and characterization of plant protein. a) The protein extraction method. b) SDS-PAGE patterns of extracted plant proteins. c) Soluble protein content of extracted plant proteins at pH 2. d) Zeta potential of extracted plant proteins at pH 2.

protein content is high, ≈20 wt%, with the majority of it being the globulin storage proteins legumin and vicilin.[29] As reported, protein contents of oilseeds are considerably higher than those of cereals. Pumpkin seed contains a large amount of protein (≈35 wt%),[30] and can reach up to 50–60 wt% in pumpkin seed residue press cake after pumpkin seed oil extraction; whereas, the protein content in proso millet is ≈13 wt% with the advantage of containing no potentially allergenic gluten.[31] The rather non-conventional protein sources, that is, pseudocereals, consisting of 10–20 wt% protein content, have attracted considerable interests due to the high nutritional value of their amino acids profile.[32] According to existing literature[33] and our previous research,[28] the legume proteins (i.e., kidney bean, black bean, cowpea, mung bean, chickpea, and lentil) can be extracted at pH 8. Meanwhile, the cereals (millet),[34] oilseeds (pumpkin seed),[35] and pseudocereals (chia seed, quinoa, and buckwheat)[27,36] can be extracted at pH 10.[37] As expected, the protein yields of legumes and oilseeds (8–21 wt%) were higher than those of cereals and pseudocereals (3–11 wt%) in this work. In addition, the protein content of extracted legumes and oilseeds protein (79–97%) was higher than those of cereals and pseudocereals (74–90%) (Figure S1, Supporting Information).

Sodium dodecyl sulphate-polyacrylamide gel electrophoresis (SDS-PAGE) results under reducing conditions, as depicted in Figure 1b, showed that the dominant globular protein in black bean, kidney bean, cowpea, and mung bean is ≈40–50 kDa. This is clearly attributable to the polypeptides of vicilin (7S or 8S).[38] The less dominant globulins at ≈30 and ≈20 kDa with low band intensity are polypeptides of legumin (11S).[39] The major subunit in chickpea is the 11S polypeptide. Lentil protein is composed of several subunits, including 7S and 11S polypeptides.[28] In the cases of pumpkin seed and quinoa, the major component is 11S-type globulins cucurbitin[40] and chenopodin,[41] respectively, accompanied by 2S albumin (10–15 kDa). Cucurbitin and chenopodin are similar to legumin protein, with both containing disulfide linked acidic (37 kDa) and basic bands (20 kDa). In addition, similar to other cereals protein, quinoa protein also contains a minority fraction of prolamin and glutelin.[42] A wide range of polypeptides with different molecular weights was observed in millet, chia, and buckwheat protein, due to the complex composition of albumin, globulin, prolamin, and glutelin.[43] As reported, legumin hexamers (320–400 kDa) have a more compact structure, higher molecular weight, and higher denaturation temperature compared with vicilin trimers (150–200 kDa).[44]

The solubility and zeta potential at pH 2, reflecting the soluble protein content and surface charge density, normally show an influence on protein self-assembly during fibrillization.[4] In Figure 1c,d, the solubility of plant proteins ranged from 58% to 89%, and the millet protein possessed the lowest solubility (58%) among these samples. Furthermore, the millet protein assembled into short fibrillar aggregates after heating (Figure S3, Supporting Information), indicating that the protein with lower solubility is not prone toward fibril formation. The zeta potential of plant proteins ranged from 3 to 33 mV at pH 2, and proteins from pseudocereals (i.e., buckwheat and chia seed) presented low charge density (3–6 mV). No fibrillar structures were observed in the proteins from buckwheat and chia seed post-incubation (Figure S3, Supporting Information), suggesting that the positive surface charge played an important role in fibril formation. In addition, only a few fibrillar aggregates were formed in quinoa protein after fibrillization (Figure S3, Supporting Information), probably due to the complexity of subunit composition. Consequently, the proteins from cereals and pseudocereals showed no significant fibrillar assemblies after heating, indicating that these proteins are unsuitable for fibrillization. We thus hypothesized that the protein from legumes and oilseeds are good candidates for manufacturing amyloid fibrils at commonly used acidic conditions.

2.2. Morphological Characterization and Statistical Analysis of Plant Protein Amyloid Fibrils

As shown in Figure S2, Supporting Information, the extracted proteins were ultrasonically treated for 15 min prior to incubation with the universal fibrillization process (pH 2, 90 °C, and stirring speed of 300 rpm), under which condition the proteins normally showed good solubility due to their positive charge. This process assists in efficiently converting the initiating protein monomers into amyloid fibrils. The mechanism of fibrillization is well understood and common to multiple proteins, consistent with previous studies on β-lactoglobulin,[45] lysozyme,[46] and oat.[23] During this process, the proteins are unfolded and hydrolyzed into polypeptides. The electrostatic repulsion between positively charged polypeptides facilitates the self-assembly of well-ordered fibrils.[47] During fibrillization, the typical cross β-sheet structure forms by β-strands oriented orthogonal to the fibrils axis, and stabilized by intermolecular hydrogen bonding.[4,9] Besides, additional forces such as the hydrophobic interaction and van der Waals forces also contribute to the fibril formation. The morphology of fibrils at the molecular level was probed using single-molecule techniques, including atomic force microscope (AFM) and transmission electron microscope (TEM), as seen in **Figure 2**a,b and Figure S3, Supporting Information. It was observed that curly and worm-like fibrils appeared for kidney bean, black bean, cowpea, and mung bean, while the proteins from chickpea, lentil, and pumpkin seed assembled into long and straight fibrils after incubation. Herneke et al. produced amyloid fibrils from a broad range of plants, and found that the formation of amyloid fibrils with a curly or straight shape was dependent on different plant sources.[15] Our findings on cowpea and chickpea agree well with those of our previous studies.[28] A curly structure of mung bean[15] and kidney bean[38] amyloid fibrils was also reported in the literature. In the case of lentil protein, flexible or semiflexible fibrils were investigated in our and others' previous studies,[28,48] probably due to composition complexity (coexisting 7S and 11S) and differences in incubation conditions. As shown in Figure S3, Supporting Information, the proteins from quinoa, millet, buckwheat, and chia seed showed no significant fibrillar protein assemblies after heating. This could be explained by the complex source composition of proteins resulting in a wide range of polypeptides with different molecular weights after hydrolysis, inducing a

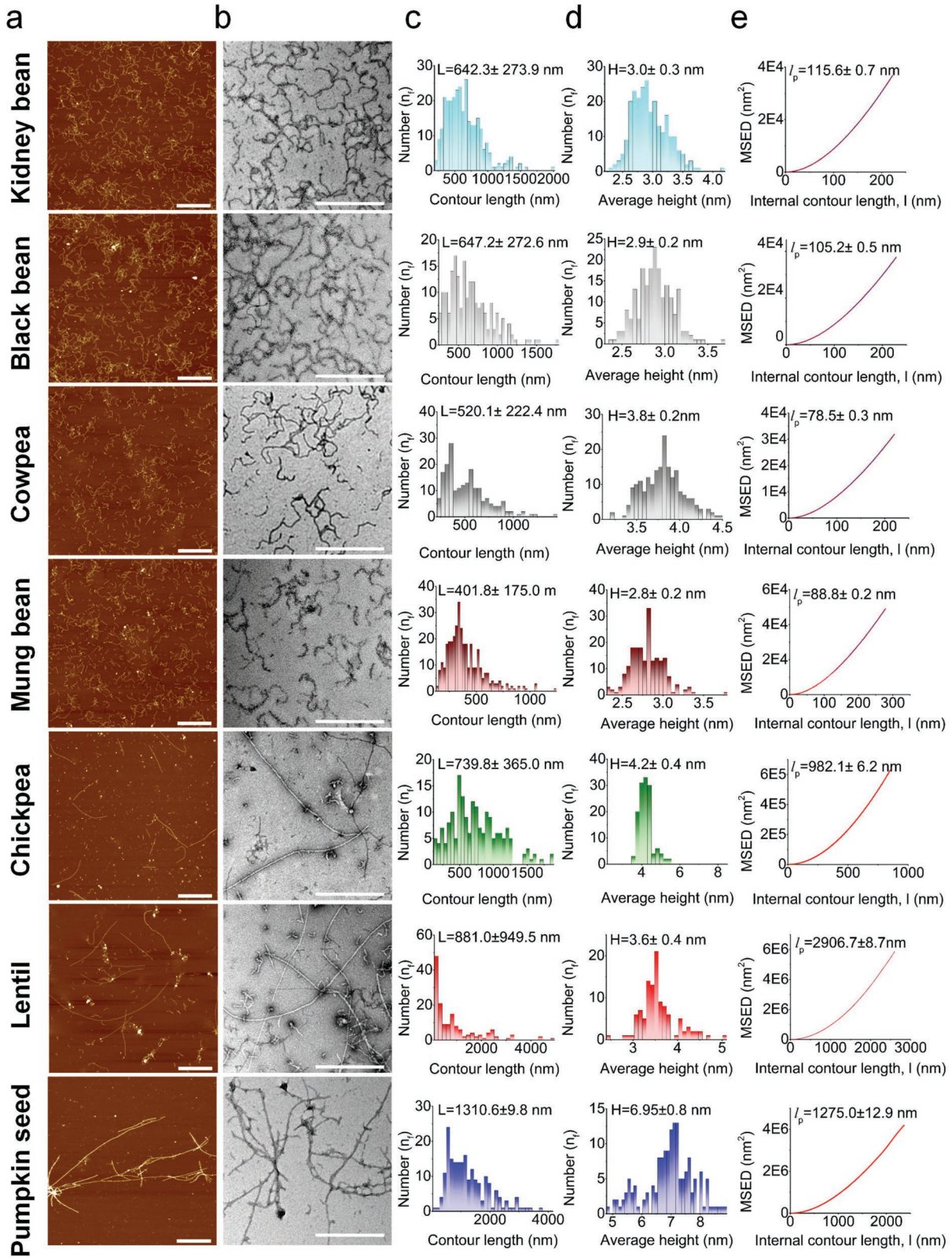

Figure 2. AFM and TEM images and statistical analysis of plant proteins after incubation at optimal fibrillization conditions (additional details can be found in Experimental Section). a) AFM images. b) TEM images. The scale bar in images represents 400 nm. c) Contour length distribution. d) Height distribution. e) Persistence length extracted from fits of mean-squared end-to-end distance (MSED) versus contour length.

different solubility in acidic solution and different susceptibility to hydrolysis during fibrillization.[10a] This phenomenon posed a negative effect on the exposure of fibrillization-prone segments and fibrils formation. In addition, the low positive charges on the surface of buckwheat and chia seed proteins also inhibited the fibrils assembly. The structural basis of amyloid formation is an amylogenic core sequences, which has to be accessible for the alignment of β-sheet structures. Even though Goldschmidt et al. demonstrated that almost all proteins contain a short sequence for forming fibrils,[3] for proteins with complex composition the suitable conditions are not clear yet.[10a] Finally, we focused on seven species of mature plant amyloid fibrils (i.e., kidney bean, black bean, cowpea, mung bean, chickpea, lentil, and pumpkin seed) to conduct further statistical analysis (Figure 2c–e).

Statistical analysis of AFM images on plant based amyloid fibrils was performed in order to elucidate the underlying mechanism of amyloid fibrils formation. Considering the convolution effect of the AFM tip, cross-section for height measurement and contour length analysis were carried out for those amyloid fibrils. The height distribution is associated with the formation of multistranded amyloid fibrils. The individual protofilaments twist around each other to form multistranded fibrils with different populations. Some amyloid fibrils populations with a height of ≈3–4 nm were observed, for example, kidney, black bean, cowpea, mung bean, chickpea, and lentil (Figure 2d), which agrees well with the most frequently occurring population of β-lactoglobulin fibrils.[49] Interestingly, the thicker fibrils with two families with an average height of 5 and 7 nm were observed in pumpkin seed fibrils, which is related to the number of packed filaments in the fibrils (Figure 2d). However, no clear periodic fluctuations along their contour length were observed among these fibrils. In addition, the flexible fibrils and rigid fibrils are defined by the statistical analysis of AFM images. According to previous studies, the persistence length is an important property of amyloid fibrils, which quantifies their rigidity.[50] As shown in Figure 2c, proteins from kidney bean, black bean, cowpea, and mung bean yielded fibrils with an average length of 400–600 nm after heating. Meanwhile, these curly fibrils exhibited a persistence length of ≈80–100 nm (Figure 2e), which identified as highly flexible fibrils. Straight and long fibrils were found in chickpea, lentil, and pumpkin seed, which elongated up to an average length of 700–1300 nm, with a persistence length reaching up to ≈1–3 μm, which is similar to β-lactoglobulin fibrils, and thus identified as rigid fibrils.[23]

As previously reported, a faster polypeptide hydrolysis rate was observed in vicilin fractions compared to legumin fractions during heating at an acidic condition.[21b,28] Therefore, we postulated that the proteins composed mainly of the vicilin (7S or 8S) fraction with lower denaturation temperatures (69–73 °C)[44,51] were hydrolyzed to small peptides during fibrillization with lower energy gain, and then assembled into short and flexible fibrils. However, proteins dominant in legumin (11S) proteins with higher denaturation temperatures around 76–77 °C[52] had larger energy gain to release building blocks during fibrillization, and then formed longer and rigid fibrils, which also agrees well with our previous studies.[28]

2.3. Structural Characterization and Comparison of Plant Protein Amyloid Fibrils

The thioflavin T (ThT) fluorescence assay is a sensitive and efficient technique to probe the formation of amyloid fibrils due to the specific binding sites with the cross β-sheet structure.[53] As shown in **Figure 3**a, ThT intensity in all protein samples was characterized by a gradual increase with incubation time, reflecting the formation of a β-sheet structure during fibrillization. The amyloid fibrils prepared from mung bean, kidney bean, and cowpea had a relatively high ThT intensity, indicating the formation of protein amyloid fibrils, in line with previous studies which have reported the formation of protein nanofibrils from these three proteins.[15,28,54] However, the ThT signal of some proteins decreased after reaching the maximum signal value. For instance, the ThT intensity of protein from kidney bean, black bean, cowpea, and mung bean achieved the maximum signal at a heating time of 10 h and then decreased with prolonged heating time. In addition, pumpkin seed protein reached the maximum ThT signal at a heating time of 6 h and then reduced gradually during the following heat treatment. The phenomenon of ThT signal loss is probably due to the disintegration of fibrils structure under excessive acid hydrolysis or the surface of the β-sheet structure being partially covered by the stacked fibrillar aggregation.[28] It was also found that there was no significant decrease of ThT intensity in chickpea and lentil during incubation, which could be due to a strong energetic driving force maintaining the linear growth of fibrils.

The circular dichroism (CD) spectra of protein before and after incubation are shown in Figure 3b. For kidney bean, black bean, cowpea, and mung bean, ellipticity at 218 nm distinctly increased, indicating the increase of β-sheet structure, which agrees well with the CD spectra of purified fibrils for mung bean and soy bean.[15] However, the ellipticity at 218 nm of chickpea, lentil, and pumpkin seed decreased slightly, which is probably attributable to the released peptides incorporated into the final fibril solution during evolution. Furthermore, the negative minimum in CD spectra shifted to around 200 nm, indicating unfolded polypeptide chains from released peptides during fibrillization. This phenomenon demonstrated that not all released peptides converted into amyloid fibrils.[55]

The typical structure of amyloid fibrils is also highlighted by Fourier-transform infrared spectroscopy (FTIR) (Figure 3c). The secondary structure was confirmed by the amine I band (1600–1700 cm^{-1}), attributed to C=O stretching, extracted from ATR-FTIR spectra, which is sensitive to the hydrogen bonds of proteins.[56] The adsorption peak of plant protein shifted to a lower wavelength (Figure 3c) after heating, demonstrating the secondary structure transition during fibrillization and the contribution of hydrogen bonds in protein assembly. As shown in **Figure 4**f, the spectral signature of almost all proteins, excluding pumpkin seed, shifted from 1630–1636 cm^{-1} to a lower frequency (1622–1626 cm^{-1}), revealing the transformation of native β-sheet in proteins to the typical parallel β-sheet structure in amyloid fibrils.[57] A similar result was also found in oat-plant-based fibrils.[23] The adsorption peak in pumpkin seed, however, shifted slightly from 1639 to 1637 cm^{-1}, and pumpkin seed had a lower ThT intensity and ellipticity intensity at 218 nm after fibrillization (Figure 4d,e). This suggested that

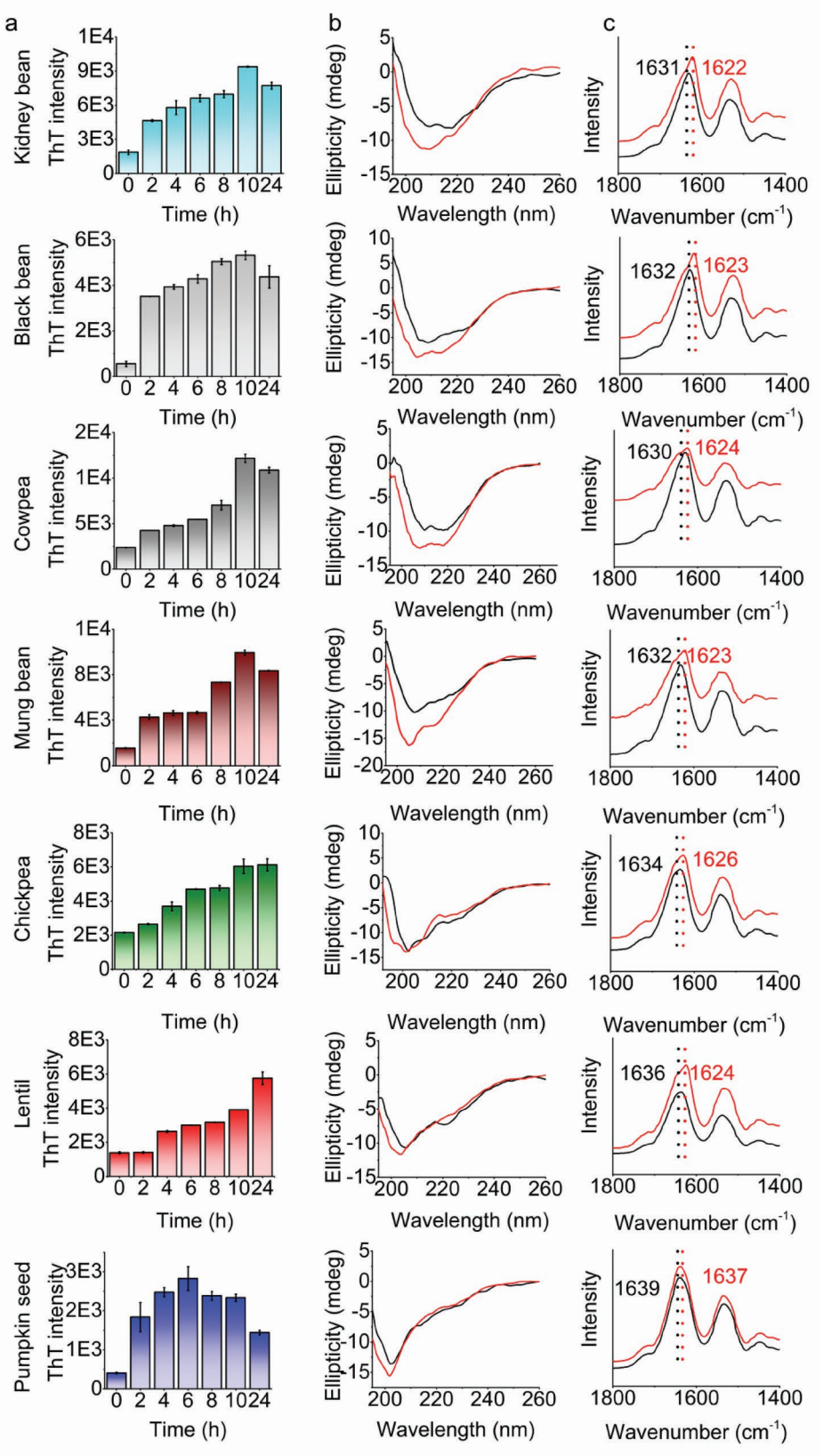

Figure 3. Structural characterization of plant proteins during fibrillization. a) ThT intensity. b) CD spectra. c) ATR-FTIR spectra. The black line reflects the plant protein before heating, and the red line represents the plant protein after incubation at optimal fibrillization conditions (additional details can be found in the Experimental Section).

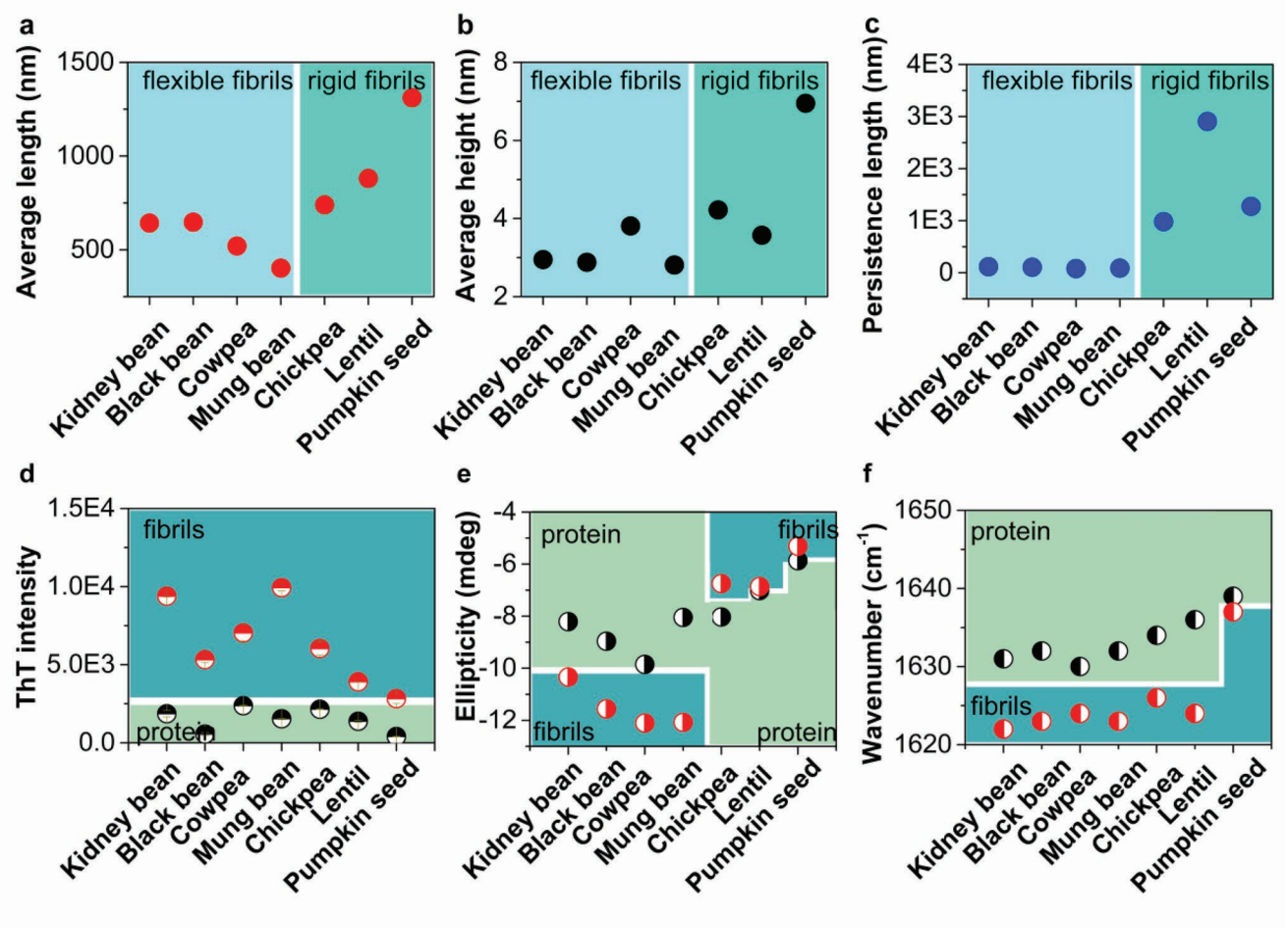

Figure 4. Comparison of a) average length, b) average height, and c) persistence length between flexible (left) and rigid (right) fibrils in each plot. Comparison of d) ThT intensity, e) ellipticity at 218 nm, and f) ATR-FTIR wavenumber shift of amide I band between plant proteins (black) and fibrils (red) in each plot.

there was a lower β-sheet content increment of pumpkin seed fibrils compared to other samples, which is in accordance with the AFM and TEM results. We also characterized the structure of fibrils using wide angle X-ray scattering (WAXS), in which a typical fiber scattering pattern at 4.51 and 9.88 Å is depicted (Figure S4, Supporting Information), further confirming the formation of amyloid fibrils.[58]

As shown in Figure 4a–c, the flexible fibrils possessed a lower average length (≈500 nm), height (3–4 nm), and persistence length (≈100 nm) when compared to rigid fibrils with a higher height (4–7 nm) and a persistence length of several micrometers. Furthermore, a higher β-sheet structure content was observed in flexible fibrils compared to rigid fibrils, as confirmed by ThT intensity and ellipticity at 218 nm in CD spectra (Figure 4d,e). This phenomenon is in agreement with morphological characterization, in which the fibrils density of flexible fibrils was higher than that of rigid fibrils, while some non-amyloid structures were incorporated into the final rigid fibrils solution, thus diluting the β-sheet content (Figure 2a,b).

The surface hydrophobicity and net charge of proteins before and after fibrillization were also determined (**Figure 5**). As shown in Figure 5a, the surface hydrophobicity of protein from kidney bean, black bean, cowpea, and mung bean increased obviously after heating, which might arise from the exposure of hydrophobic amino acid side chains during unfolding and hydrolysis. However, a decreasing trend was observed in chickpea, lentil, and pumpkin, possibly due to the buried hydrophobic patches during protein assembly.[59] This phenomenon could be ascribed to the exposed hydrophobic patches more likely existing on the surface of short flexible fibrils; whereas, hydrophobic patches aligned inside of the amyloid core during the formation of long and rigid fibrils. As depicted in Figure 5b, the zeta potential of all protein samples increased after heating, indicating that the increased positive charge density favored inter-fibril aggregation. The surface charge density of amyloid fibrils from chickpea and lentil was higher than that of other samples. This suggested that the strong electrostatic repulsion favored the linear growth of building blocks during fibrillization, which explained the continuous increase of ThT signal of chickpea and lentil in Figure 3a.

2.4. Multifunctional Sustainable Applications of Plant Protein Amyloid Fibrils

Amyloid fibrils have been proven to be an excellent candidate for templating various materials and biotechnological

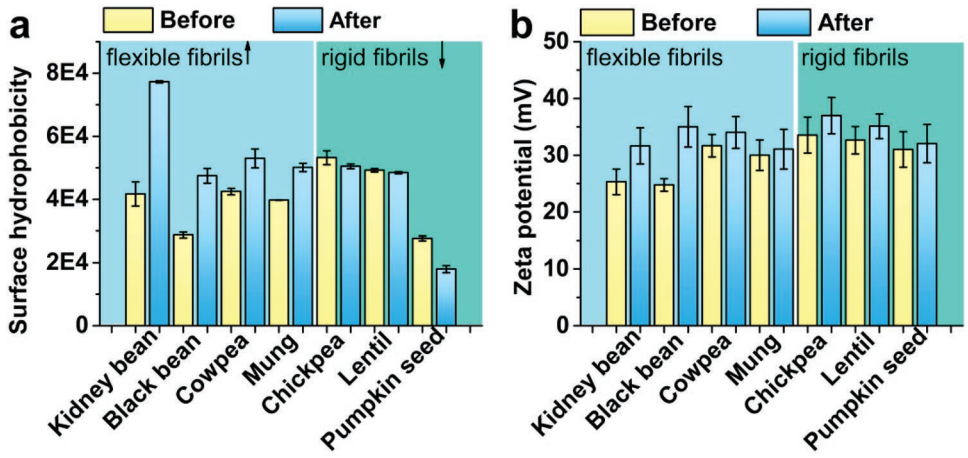

Figure 5. a) The surface hydrophobicity and b) zeta potential of plant proteins before and after incubation at optimal fibrillization conditions (additional details can be found in Experimental Section).

applications.[5] In this work, we applied plant protein amyloid fibrils as functional materials for applications, including hydrogel fabrication, bioplastics film production and membranes for water purification, as shown in **Figure 6**. Recently, hydrogels have been used for multiple purposes, including for example, drug release in biomedical applications and nutraceutical delivery vehicles,[11,60] Because of the existence of non-amyloid structures in the final rigid fibrils solution (Figure 3b), fibrils based on chickpea, lentil, and pumpkin seed fibrils cannot form gel networks during ion-induced gelation. However, we can fabricate hydrogels using amyloid fibrils from kidney bean, black bean, cowpea, and mung bean because of a high fibrils content in these flexible fibrils at a fixed protein concentration (Figure 2a). As shown in Figure 6a, scanning electron microscopy (SEM) images of dried hydrogel revealed that the hydrogel networks were composed of a physical entanglement of flexible fibrils with high compactness driven by electrostatic forces. In line with the statistical length distribution (Figure 2), the mesh size of black-bean-based gels was larger than that of the other samples, with the smallest mesh size observed in mung-bean-based gels (Figure 4a). The compactness of networks from plant protein amyloid fibrils based gels was higher than that of β-lactoglobulin amyloid fibrils,[61] which are attributable to the difference of contour length and flexibility of fibrils.

As a result of raising environmental concerns about plastic pollution, protein and biodegradable polymer hybrid bioplastics have attracted tremendous attention due to their sustainable properties.[24,62] Figure 6b shows smooth hybrid bioplastics films made of plant amyloid fibrils blended with the biodegradable polymer polyvinyl alcohol (PVA), and a plasticizer (glycerol). The weight ratio of plant fibrils, PVA and glycerol is 4:3:3, the same ratio used in earlier literature.[62] Consequently, the plant fibrils are the main component of the blend and give a high contribution to mechanical properties of the resulting bioplastics. Furthermore, amyloid fibrils provide functionalities such as UV screening and antioxidant properties, that PVA cannot provide; however, the bioplastics films are brittle without PVA, which essentially has a toughening role.[62] Our aim here is to compare their performance for various protein fibrils with a fixed blend composition. The mechanical properties of hybrid films are presented in Figure 6c. In stress–strain curves, various plant amyloid fibrils exhibited dissimilar behaviors, arising from the differences in the fibrils structure and their amount in final solution. The elongation at break of plant fibrils based bioplastics ranged from 1000% to 1300% (Figure S5a, Supporting Information). Tensile strength was ≈5–8 MPa, as shown in Figure S5b, Supporting Information. Among rigid fibrils, the Young's modulus of pumpkin seed fibrils hybrid bioplastics was higher than chickpea and lentil fibrils, which could be attributed to the longer average length and thicker height of pumpkin seed fibrils compared to that of chickpea and lentil fibrils (Figure 2). However, pumpkin seed achieved the minimum value of ultimate elongation (715.83%) and break stress (4.86 MPa). In addition, some events of fracture and fragmentation can be seen from the protruding points on the stress–strain plot of pumpkin seed hybrid films (Figure 6c). This phenomenon suggested that the film fabricated by amyloid fibrils from pumpkin seed was more easily broken compared to other samples, probably due to the lower β-sheet content and fibrils content. Black bean amyloid fibrils hybrid bioplastics film exhibited excellent performance in elongation, which is ascribed to the good alignment of flexible fibrillar structures against the deformed forces. The initial slope of stress–strain curves was used to determine the Young's modulus, as seen in Figure 6d. The flexible fibrils hybrid films showed a higher Young's modulus and higher elongation rate than those formed by rigid fibrils, probably due to the entanglement of dense flexible fibrils through physical interactions.[62] Among flexible fibrils, kidney bean fibrils (13.53 MPa) and black bean fibrils (16.51 MPa) presented higher Young's modulus than cowpea and mung bean fibrils, which could be attributable to the higher average length of kidney bean and black bean fibrils (642–647 nm) than cowpea and mung bean fibrils (401–520 nm), yet lower than bioplastics based starting from animal amyloid fibrils.[62] Moreover, the tensile property and Young's modulus of black bean fibrils structured film were observed to be superior to those of other samples because of the higher intermolecular interactions and arrangement of fibrillar structures. Taken together, a lower Young's modulus and a higher elongation to

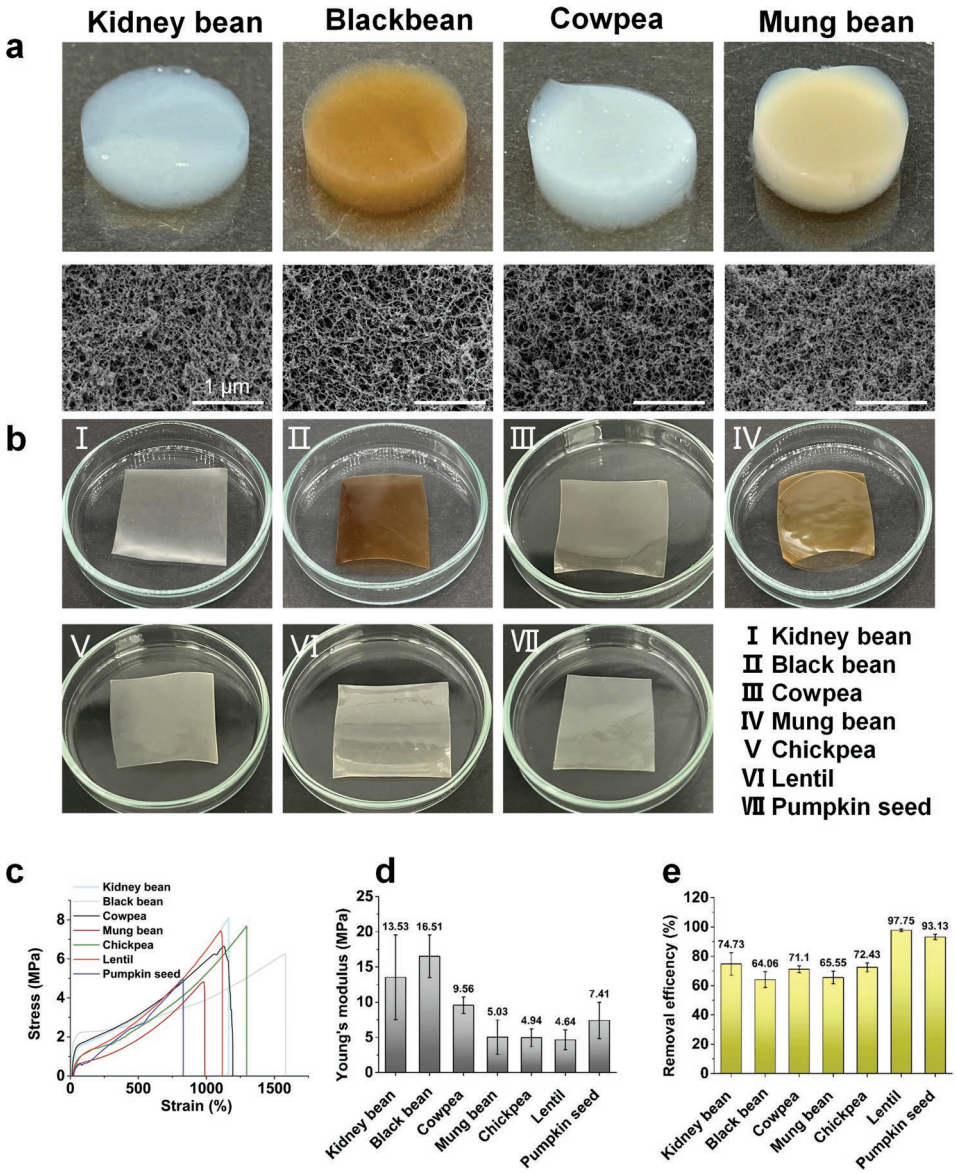

Figure 6. Multifunctional sustainable applications of plant-protein-based fibrils. a) Hydrogel images and SEM images of kidney bean, black bean, cowpea, and mung bean protein-based fibrils. b) Bioplastics samples. c) Stress–strain curves of bioplastic films. d) Young's modulus of bioplastics films. e) Gold removal efficiency of plant protein fibrils-carbon hybrid membranes.

break were obtained here starting from plant-based amyloid fibrils hybrid bioplastic films compared to bioplastics starting from animal amyloid fibrils,[62] suggesting a behavior similar to that of synthetic elastomers.

In order to address global water pollution, amyloid fibrils can be used as an efficient superabsorbent due to their excellent properties and adsorption affinity.[24,63] Plant amyloid-fibrils-based membranes for heavy metal removal from water were fabricated. In our previous publication, we showed and discussed in details the selectivity of amyloid fibrils toward different ions.[63] The primary mechanism for the adsorption of heavy metals by protein nanofibrils is metal–ligand chelation, for which the adsorption energy is in the order of 10 to 100 $K_B T$;[64] accordingly the metals with higher atomic numbers, such as gold and palladium, are better adsorbed compared to light metals such as sodium and potassium, for which the binding constant is lower. Therefore, gold was used as a model heavy metal pollutant to explore the potential of various plant amyloid fibrils for water purification. As shown in Figure 6e, high removal efficiencies (64–97%) were achieved by hybrid membranes composed of plant fibrils and activated carbon. Furthermore, the rigid fibrils from lentil and pumpkin seed achieved higher performance (>90%) in gold removal. This excellent removal efficiency is comparable to that of hybrid membranes composed of oat globulin or β-lactoglobulin amyloid fibrils-activated carbon.[63,65] The higher amount of cysteine in legumin-based rigid fibrils than vicilin[25b] also favored metal chelation between the thiol groups from cysteine and heavy metals.[63] In addition, the carboxyl moieties from abundant aspartic acid and glutamic acid reduced the heavy metal

content in polluted water through electrostatic interaction. As illustrated in Figure S6b, Supporting Information, after filtration by rigid amyloid fibrils-activated carbon hybrid membranes, the lentil fibrils achieved the lowest gold concentration, which decreased from 527 to 11 ppb. Moreover, the individual performance of pure amyloid fibrils for higher gold concentration (10 ppm) removal was analyzed, as shown in Figure S6a, Supporting Information. We previously reported that the adsorption capacity of pure activated carbon membrane in the same conditions is 0.3 mg g^{-1} for gold.[66] As shown in Figure S6, Supporting Information, the gold adsorption capacity of pure plant amyloid fibrils is 62–88 mg g^{-1}, which is 200 times higher than that of activated carbon. Furthermore, it was found that the adsorption capacity of rigid amyloid fibrils (78.1–88.6 mg g^{-1}) was superior to that of flexible fibrils (62.6–83.4 mg g^{-1}), which is comparable to that of sunflower and peanut fibrils.[67]

In aggregate, flexible fibrils with high density can form a gel network structure through electrostatic forces during ion-induced gelation. Furthermore, the flexible fibrils hybrid films exhibited higher mechanical performance than rigid fibrils, which is attributed to a strong interfibrillar interaction against deformation. In addition, the heavy metal removal efficiency of rigid fibrils was superior to that of flexible fibrils, due to the chemical and physical bonding between specific amino acid groups and heavy metals. The amyloid fibrils from a variety of plant sources achieved excellent performance in different functional materials, which provided novel insight into the rational design and application of fibril structures.

3. Conclusion

In this work, a wide range of sustainable and low-cost plant proteins, including legumes, cereals, oilseeds, and pseudocereals, were extracted using an efficient and universal protocol, and successfully manufactured rigid and flexible amyloid fibrils. The proteins from legumes and oilseeds for fibrillization were superior to those of cereals and pseudocereals due to the higher solubility and surface charge. It was also revealed that the proteins dominant in the vicilin fraction (7S or 8S) were prone to be hydrolyzed into small peptides during fibrillization, assembling into short and flexible fibrils with a persistence length of ≈100 nm. Proteins consisting mainly of legumin (11S) showed a high propensity of forming longer and rigid fibrils with a persistence length of several micrometers. Moreover, a higher β-sheet structure content was observed in flexible fibrils compared to that in rigid fibrils. Flexible fibrils exhibited good performance on hydrogel and bioplastics film fabrication, while rigid fibrils presented better efficiency in heavy metal removal, which promoted the rational design of amyloid fibrillar structures for optimal tailoring of potential applications. Overall, these results indicated the potential application of plant protein amyloid fibrils in future sustainable materials.

4. Experimental Section

Plant Protein Extraction: The proteins from legumes, cereals, oilseeds, and pseudocereals were extracted using the method of alkaline solution and acid precipitation (AE-IP), according to previous studies.[25] First, kidney bean, black bean, cowpea, mung bean, chickpea, lentil, millet, buckwheat, pumpkin seed, quinoa, and chia seed were milled to powder. Then, the plant flour was defatted three times by hexane at a ratio of 1:10 for 4 h each time. After defatting, the plant flour was dried using a fume hood for 12 h. Subsequently, the plant flour was dispersed in Milli-Q water at a ratio of 1:10 w/v, and then the pH of the dispersion was adjusted to pH 8–10 using 4 M NaOH. For kidney bean, black bean, cowpea, mung bean, chickpea, and lentil, the dispersion was adjusted to pH 8, and for millet, buckwheat, pumpkin seed, quinoa, and chia seed, the dispersion was adjusted to pH 10. After stirring for 2 h, these dispersions were centrifuged at 10 000 × *g* for 15 min. The resultant supernatant was adjusted to pH 4.5 using 4 M HCl, and then centrifuged at 10 000 × *g* for 15 min. The collected precipitates were then re-dispersed into Milli-Q water and re-adjusted to pH 7. After dialysis for 2 days, the protein solution was freeze-dried for 3 days to collect the protein powder.

Plant Protein Fibrils Production: The plant proteins were dispersed in pH 2 Milli-Q water to a concentration of 3 wt%, and then the pH of the dispersion was adjusted to pH 2. The dispersion received ultrasonic treatment for 20 min, and was subsequently centrifuged for 15 min at 10 000 × *g*. The resultant supernatant was incubated at 90 °C with an oil bath, and the stirring speed was 300 rpm. According to AFM images with different heating times, the optimized incubation time for kidney, black bean, mung bean, chickpea, and lentil protein was 10 h, for cowpea protein was 8 h, and for pumpkin seed protein was 6 h. After heating, the amyloid fibrils were cooled with an ice bath and stored at 4 °C for further analysis.

SDS-PAGE: The plant proteins were dissolved in Laemmli buffer with 10% DL-dithiothreitol (reducing condition) to the concentration of 2 mg mL^{-1}, and then heated at 100 °C for 5 min. Then, the marker and samples were loaded on gels (4–20% Criterion TGX Stain-Free Protein Gel) with the voltage of 200 V. After 40 min, the gels were taken out and imaged using a gel imaging system (ChemiDoc MP, Bio-Rad, U.S.A.).

ThT Fluorescence Spectroscopy: To prepare ThT stock solution (2 mM), the ThT powder was dissolved in Milli-Q water and filtered with a 0.22 μm syringe filter to remove insoluble precipitates. Then, the ThT working solution (20 mM) was generated by diluting the ThT stock solution 100 times using Milli-Q water. During fibrillization, 10 μL of sample solution was taken out and mixed with 190 μL ThT working solution, and then transferred to a 96-well microplate. Afterward, the ThT fluorescence intensity of fibrillated samples was measured by an Infinite M200 pro plate reader (Tecan Group AG, Switzerland) with the excitation wavelength of 440 nm and emission wavelength of 480 nm. Finally, the ThT intensity of samples was corrected by subtracting the background of ThT working solution.

ATR-FTIR: The protein and amyloid fibrils from different plants were placed on top of the ATR crystal, and scanned from 4000 to 600 cm^{-1} with the resolution of 4 cm^{-1} using a Varian 640 FTIR spectrometer (ThermoFisher Scientific, U.S.A.). Each sample was scanned 64 times. The peak position of amide I band (1700–1600 cm^{-1}) was analyzed and displayed in this work.

CD Spectroscopy: The protein and amyloid fibrils were diluted to the concentration of 0.1 mg mL^{-1}, and then transformed into a quartz cell with a 1 mm path length. The CD spectra of samples were collected from 260 to 190 nm using a Jasco J-815 CD spectrometer.

WAXS: The lyophilized amyloid fibrils samples were used for the WAXS experiment. The experiment was performed with the scattering vector q from 0.2 to 2 $Å^{-1}$ ($q = \frac{4\pi}{\lambda}\sin\frac{\theta}{2}$, θ is the scattering angle) by using a Rigaku micro-focused source equipped with Cu Kα radiation. The corresponding distance was calculated according to $d = \frac{2\pi}{q}$. The collected WAXS signal was analyzed by an imaging system (Fujifilm BSA-MS 2025). The powder samples were packed in 2 mm capillaries. The scan time was 15 h per sample.

Zeta Potential: The protein and amyloid fibrils were diluted to the concentration of 1 mg mL^{-1} using pH 2 Milli-Q water. Then, 1 mL

solution was transferred to disposable folded electrophoresis cells (DTS1070) and measured using the Malvern Zetasizer Nano ZS. The experiment parameters were equilibration time of 60 s and scattering angle of 173°. Each experiment was repeated in triplicate.

Surface Hydrophobicity: The protein and amyloid fibrils were diluted to a concentration ranging from 0.1 to 0.5 mg mL^{-1} with pH 2 Milli-Q water. A 5 µL sample was mixed with 200 µL ANS (80 µM) in a 96-well plate, and then measured using a Tecan plate reader with an excitation of 390 nm and emission of 484 nm. The surface hydrophobicity was calculated by the slope of the fluorescence intensity versus the concentration of samples.

AFM and Data Analysis: The amyloid fibrils solutions were diluted to 0.1 wt% using pH 2 Milli-Q water. Subsequently, a drop (10 µL) of diluted solution was deposited on freshly cleaved mica and incubated for 2 min. Afterward, the mica was rinsed by pH 2 Milli-Q water and dried with compressed air flow. The AFM images were captured using a Bruker Multimode 8 microscope in tapping mode at room temperature. Finally, the collected images were flattened using Nanoscope Analysis version 1.40 and then statistically analyzed by FiberApp.[50]

TEM: The diluted amyloid fibrils solutions (0.1 wt%) were spread onto a glow discharged copper grid and incubated for 1 min. Then, the grid was rinsed twice with Milli-Q water and stained twice by uranyl acetate for 10 s. Subsequently, the grid was dried under ambient conditions, and then inserted to the Morgagni 268 electron microscope for imaging with an acceleration voltage of 100 kV.

Amyloid Fibrils Prepared Hydrogel and Characterization: To prepare hydrogel, 2 wt% amyloid fibrils dispersion was dialyzed for 2 days with the 0.3 M NaCl solution. After collecting hydrogel samples, the water in hydrogels was replaced by pure ethanol and then dried using a supercritical CO_2 drying instrument (Tousimis Autosamdri 931). The microstructure of the dried hydrogel was observed by SEM. Small pieces of the dried gels were mounted on SEM aluminum stubs in conductive carbon paint (Plano, DE, U.S.A.), and after drying, carefully fractured with a razor blade. The samples were sputter-coated under rotation at an angle of ≈20° with 5 nm of platinum/palladium (CCU-10, Safematic, CH). The images were recorded at a working distance of ≈4–5 mm with a SEM (Merlin, Zeiss, DE) operated at an accelerating voltage of 1.5 kV.

Amyloid Fibrils Prepared Membrane for Water Purification: The pure amyloid fibrils, in combination with activated carbon, were used for membrane preparation in water purification. For pure amyloid fibrils membrane, 1 mL of 0.2 wt % dispersion was deposited on the surface of cellulose filters by vacuum filtration. For hybrid membrane, the mixture of 1 mL amyloid fibrils dispersion (2 wt%) and 2 mL activated carbon (10 wt%) was filtered on the surface of cellulose filters using vacuum filtration to prepare the composite membranes. Subsequently, the gold concentration of the original solution and filtrates was measured by using an AA240Z graphite-furnace atomic absorption spectroscopy. The removal efficiency was measured using gold solution with a concentration of 500 ppb and amyloid-activated carbon hybrid membrane. A higher gold concentration of 10 ppm and pure amyloid fibrils membrane was used to determine the adsorption capacity. The removal efficiency (E) and adsorption ability (q) were calculated by Equations (1) and (2), respectively

$$E = \left(1 - \frac{C_p}{C_f}\right) \times 100\% \quad (1)$$

$$q = \frac{\left(C_p - C_f\right) \times V}{m} \quad (2)$$

where C_p and C_f are the concentration of permeate streams and original solution, respectively; V is the volume of gold solution after filtration (L); and m is the weight of amyloid fibrils (g).

Amyloid Fibrils Fabricated Bioplastics Film and Characterization: The hybrid amyloid fibrils films were prepared by mixing amyloid fibrils (2 wt%), PVA (1.5 wt%), and glycerol (1.5 wt%). The weight ratio of plant fibrils, PVA, and glycerol is 4:3:3, which is set according to previous studies.[62] To avoid the effects of biodegradable polymer on the fibrils formation, PVA and glycerol were added to amyloid fibrils dispersion 1 h prior to the end of fibrillization, and then heating continued at 90 °C for 1 h to dissolve PVA. After incubation, the solution was cast on a Petri dish and dried at room temperature for 2 days. The mechanical properties of bio-plastic film were measured according Peydayesh et al.[62] The stress–strain curves were collected using a Z010 (Zwick) with a 100 N load cell, which was also used for calculating Young's modulus. This experiment was repeated in triplicate.

Supporting Information

Supporting Information is available from the Wiley Online Library or from the author.

Acknowledgements

T.L. and J.Z. contributed equally to this work. The authors thank Jie Teng for productive ideas on this work, and Zhou Dong for assistance in the supercritical CO_2 drying experiment. The authors also thank Dr. Stephan Handschin (ETH Zurich) for assistance in SEM images, and the Scientific Center for Optical and Electron Microscopy (ScopeM) of ETH Zurich. The first author expresses gratitude for the financial support of the China Scholarship Council.

Conflict of Interest

M.B., M.P., and R.M. have filed a patent related to this article on behalf of ETH Zurich. All other authors declare no conflict of interest.

Data Availability Statement

The data that support the findings of this study are available from the corresponding author upon reasonable request.

Keywords

amyloid fibrils, bioplastics, fibrillization, plant proteins, water purification

Received: October 25, 2022
Revised: December 20, 2022
Published online: January 12, 2023

[1] F. Chiti, C. M. Dobson, *Annu. Rev. Biochem.* **2006**, *75*, 333.
[2] P. C. Ke, R. Zhou, L. C. Serpell, R. Riek, T. P. Knowles, H. A. Lashuel, E. Gazit, I. W. Hamley, T. P. Davis, M. Fändrich, *Chem. Soc. Rev.* **2020**, *49*, 5473.
[3] L. Goldschmidt, P. K. Teng, R. Riek, D. Eisenberg, *Proc. Natl. Acad. Sci. U. S. A.* **2010**, *107*, 3487.
[4] M. Mohammadian, A. Madadlou, *Trends Food Sci. Technol.* **2018**, *75*, 115.
[5] T. P. J. Knowles, R. Mezzenga, *Adv. Mater.* **2016**, *28*, 6546.
[6] S. K. Maji, D. Schubert, C. Rivier, S. Lee, J. E. Rivier, R. Riek, *PLoS Biol.* **2008**, *6*, e17.
[7] D. Men, Z.-P. Zhang, Y.-C. Guo, D.-H. Zhu, L.-J. Bi, J.-Y. Deng, Z.-Q. Cui, H.-P. Wei, X.-E. Zhang, *Biosens. Bioelectron.* **2010**, *26*, 1137.
[8] S. L. Gras, A. K. Tickler, A. M. Squires, G. L. Devlin, M. A. Horton, C. M. Dobson, C. E. MacPhee, *Biomaterials* **2008**, *29*, 1553.

[9] Y. Cao, R. Mezzenga, *Adv. Colloid Interface Sci.* **2019**, *269*, 334.
[10] a) K. J. A. Jansens, M. A. Lambrecht, I. Rombouts, M. Monge Morera, K. Brijs, F. Rousseau, J. Schymkowitz, J. A. Delcour, *Compr. Rev. Food Sci. Food Saf.* **2019**, *18*, 1256; b) M. A. Lambrecht, K. J. A. Jansens, I. Rombouts, K. Brijs, F. Rousseau, J. Schymkowitz, J. A. Delcour, *Compr. Rev. Food Sci. Food Saf.* **2019**, *18*, 1277.
[11] B. Hu, Y. Shen, J. Adamcik, P. Fischer, M. Schneider, M. J. Loessner, R. Mezzenga, *ACS Nano* **2018**, *12*, 3385.
[12] Y. Shen, L. Posavec, S. Bolisetty, F. M. Hilty, G. Nyström, J. Kohlbrecher, M. Hilbe, A. Rossi, J. Baumgartner, M. B. Zimmermann, R. Mezzenga, *Nat. Nanotechnol.* **2017**, *12*, 642.
[13] X. Jia, M. Peydayesh, Q. Huang, R. Mezzenga, *Small* **2022**, *18*, 2105502.
[14] K. Antonets, A. Nizhnikov, *Int. J. Mol. Sci.* **2017**, *18*, 2155.
[15] A. Herneke, C. Lendel, D. Johansson, W. Newson, M. Hedenqvist, S. Karkehabadi, D. Jonsson, M. Langton, *ACS Food Sci. Technol.* **2021**, *1*, 854.
[16] J. Adamcik, R. Mezzenga, *Angew. Chem., Int. Ed.* **2018**, *57*, 8370.
[17] C. C. vandenAkker, M. F. M. Engel, K. P. Velikov, M. Bonn, G. H. Koenderink, *J. Am. Chem. Soc.* **2011**, *133*, 18030.
[18] C. Schmitt, C. Bovay, A.-M. Vuilliomenet, M. Rouvet, L. Bovetto, R. Barbar, C. Sanchez, *Langmuir* **2009**, *25*, 7899.
[19] S. M. Loveday, X. L. Wang, M. A. Rao, S. G. Anema, L. K. Creamer, H. Singh, *Int. Dairy J.* **2010**, *20*, 571.
[20] Y. Cao, J. Adamcik, M. Diener, J. R. Kumita, R. Mezzenga, *J. Am. Chem. Soc.* **2021**, *143*, 11473.
[21] a) Y. Wan, S. Guo, *Recent Adv. Food Sci.* **2019**, *14*, 164; b) C.-H. Tang, C.-S. Wang, *J. Agric. Food Chem.* **2010**, *58*, 11058.
[22] T. Li, L. Wang, H. Geng, X. Zhang, Z. Chen, *Food Chem.* **2021**, *354*, 129554.
[23] J. T. Zhou, T. Li, M. Peydayesh, M. Usuelli, V. Lutz-Bueno, J. Teng, L. Wang, R. Mezzenga, *Adv. Sci.* **2022**, *9*, e2104445.
[24] M. Peydayesh, M. Bagnani, W. L. Soon, R. Mezzenga, *Chem. Rev.* **2022**, https://doi.org/10.1021/acs.chemrev.2c00236.
[25] a) Y. W. Sari, W. J. Mulder, J. P. M. Sanders, M. E. Bruins, *Biotechnol. J.* **2015**, *10*, 1138; b) J. Boye, F. Zare, A. Pletch, *Food Res. Int.* **2010**, *43*, 414.
[26] Z. Gao, P. Shen, Y. Lan, L. Cui, J.-B. Ohm, B. Chen, J. Rao, *Food Res. Int.* **2020**, *131*, 109045.
[27] G. A. Ruiz, W. Xiao, M. van Boekel, M. Minor, M. Stieger, *Food Chem.* **2016**, *209*, 203.
[28] T. Li, L. Wang, X. Zhang, H. Geng, W. Xue, Z. Chen, *Food Hydrocolloids* **2021**, *111*, 106396.
[29] R. Bou, P. Navarro-Vozmediano, R. Dominguez, M. Lopez-Gomez, M. Pinent, A. Ribas-Agusti, J. J. Benedito, J. M. Lorenzo, X. Terra, J. V. Garcia-Perez, M. Pateiro, J. A. Herrera-Cervera, R. Jorba-Martin, *Compr. Rev. Food Sci. Food Saf.* **2022**, *21*, 2200.
[30] J. M. Dotto, J. S. Chacha, *Sci. Afr.* **2020**, *10*, e00575.
[31] P. Gulati, A. Li, D. Holding, D. Santra, Y. Zhang, D. J. Rose, *J. Agric. Food Chem.* **2017**, *65*, 1952.
[32] A. M. Malik, A. Singh, *Recent Adv. Chem. Compos. Tob. Tob. Smoke, Symp.* **2022**, *1*, 100001.
[33] A. C. Karaca, N. Low, M. Nickerson, *Food Res. Int.* **2011**, *44*, 2742.
[34] F. Jhan, A. Gani, N. Noor, A. Shah, *ACS Food Sci. Technol.* **2021**, *1*, 1418.
[35] S. Bučko, J. Katona, L. Popović, Ž. Vaštag, L. Petrović, M. Vučinić–Vasić, *LWT–Food Sci. Technol.* **2015**, *64*, 609.
[36] D. N. López, R. Ingrassia, P. Busti, J. Wagner, V. Boeris, D. Spelzini, *LWT* **2018**, *97*, 523.
[37] D. N. López, M. Galante, G. Raimundo, D. Spelzini, V. Boeris, *Food Res. Int.* **2019**, *116*, 419.
[38] C.-H. Tang, Y.-H. Zhang, Q.-B. Wen, Q. Huang, *J. Agric. Food Chem.* **2010**, *58*, 8061.
[39] C.-H. Tang, X. Sun, *J. Agric. Food Chem.* **2010**, *58*, 6395.
[40] L. Rezig, F. Chibani, M. Chouaibi, M. Dalgalarrondo, K. Hessini, J. Guéguen, S. Hamdi, *J. Agric. Food Chem.* **2013**, *61*, 7715.
[41] S. Dakhili, L. Abdolalizadeh, S. M. Hosseini, S. Shojaee-Aliabadi, L. Mirmoghtadaie, *Food Chem.* **2019**, *299*, 125161.
[42] X. Wang, R. Zhao, W. Yuan, *J. Cereal Sci.* **2020**, *95*, 103036.
[43] Y. P. Timilsena, R. Adhikari, C. J. Barrow, B. Adhikari, *Food Chem.* **2016**, *212*, 648.
[44] J.-L. Session, M. L. Chihi, N. Sok, R. Saurel, *Food Hydrocolloids* **2015**, *46*, 233.
[45] S. M. Loveday, S. G. Anema, H. Singh, *Int. Dairy J.* **2017**, *67*, 35.
[46] S. E. Hill, J. Robinson, G. Matthews, M. Muschol, *Biophys. J.* **2009**, *96*, 3781.
[47] V. Foderà, A. Zaccone, M. Lattuada, A. M. Donald, *Phys. Rev. Lett.* **2013**, *111*, 108105.
[48] C. Wynnychuk, Y.-J. Jo, Y. Chu, L. Chen, *Food Struct.* **2021**, *29*, 100204.
[49] J. Adamcik, J.-M. Jung, J. Flakowski, P. De Los Rios, G. Dietler, R. Mezzenga, *Nat. Nanotechnol.* **2010**, *5*, 423.
[50] I. Usov, R. Mezzenga, *Macromolecules* **2015**, *48*, 1269.
[51] Y.-H. Zhang, C.-H. Tang, Q.-B. Wen, X.-Q. Yang, L. Li, W.-L. Deng, *Food Hydrocolloids* **2010**, *24*, 266.
[52] C. Yang, B. Wang, J. Wang, S. Xia, Y. Wu, *LWT* **2019**, *109*, 443.
[53] M. Biancalana, S. Koide, *Biochim. Biophys. Acta, Proteins Proteomics* **2010**, *1804*, 1405.
[54] J. Liu, C.-H. Tang, *Food Res. Int.* **2013**, *51*, 621.
[55] C. Akkermans, P. Venema, A. J. van der Goot, H. Gruppen, E. J. Bakx, R. M. Boom, E. van der Linden, *Biomacromolecules* **2008**, *9*, 1474.
[56] M. Mohammadian, A. Madadlou, *Food Hydrocolloids* **2016**, *52*, 221.
[57] R. Sarroukh, E. Goormaghtigh, J.-M. Ruysschaert, V. Raussens, *Biochim. Biophys. Acta* **2013**, *1828*, 2328.
[58] K. L. Morris, L. C. Serpell, in *Amyloid Proteins: Methods in Molecular Biology*, 2nd ed., Humana Press, Totowa, NJ **2012**, pp. 121–135.
[59] Z. Wei, Q. Huang, *Food Hydrocolloids* **2019**, *89*, 579.
[60] Z. Wei, Y. Chen, W. Wijaya, Y. Cheng, J. Xiao, Q. Huang, *Food Funct.* **2020**, *11*, 1478.
[61] M. Usuelli, T. Germerdonk, Y. Cao, M. Peydayesh, M. Bagnani, S. Handschin, G. Nystrom, R. Mezzenga, *Nanoscale* **2021**, *13*, 12534.
[62] M. Peydayesh, M. Bagnani, R. Mezzenga, *ACS Sustainable Chem. Eng.* **2021**, *9*, 11916.
[63] M. Peydayesh, R. Mezzenga, *Nat. Commun.* **2021**, *12*, 3248.
[64] M. R. Hammond, R. Mezzenga, *Soft Matter* **2008**, *4*, 952.
[65] J. Zhou, T. Li, M. Peydayesh, M. Usuelli, V. Lutz-Bueno, J. Teng, L. Wang, R. Mezzenga, *Adv. Sci.* **2022**, *9*, 2104445.
[66] S. Bolisetty, R. Mezzenga, *Nat. Nanotechnol.* **2016**, *11*, 365.
[67] W. L. Soon, M. Peydayesh, R. Mezzenga, A. Miserez, *Chem. Eng. J.* **2022**, *445*, 136513.